Research Article | Vol. 26, No. 14 | 9 Jul 2018 | OPTICS EXPRESS 18143
Optics EXPRESS

Non-linear adaptive three-dimensional imaging with interferenceless coded aperture correlation holography (I-COACH)

MANI R. RAI,* A. VIJAYAKUMAR, AND JOSEPH ROSEN

Department of Electrical and Computer Engineering, Ben-Gurion University of the Negev, P.O. Box 653, Beer-Sheva 8410501, Israel
**maniratn@post.bgu.ac.il*

Abstract: Interferenceless coded aperture correlation holography (I-COACH) is an incoherent digital holography technique for imaging 3D objects without two-wave interference. In I-COACH, the object beam is modulated by a pseudorandom coded phase mask (CPM) and propagates to the camera where its intensity pattern is recorded. The image of the object is reconstructed by a cross-correlation of the object intensity pattern with a point intensity response of the system, whereas the light from both the object and the point, are modulated by the same CPM. In order to recover the image of the object without bias level and background noise, multiple intensity recordings are necessary for both objects as well as the point object, which in turn significantly reduces the time resolution of imaging. In this study, a non-linear reconstruction technique is developed to reconstruct the image of the object with only a single camera shot. Furthermore, the proposed technique is adaptive to different experimental conditions in the sense of finding different optimal parameters for each experiment. The new method has been implemented on a regular I-COACH system in both transmission as well as reflection illumination modes.

OCIS codes: (090.1995) Digital holography; (110.0110) Imaging systems; (110.6880) Three-dimensional image acquisition; (090.1760) Computer holography; (050.0050) Diffraction and gratings.

References and links

1. T.-C. Poon and J.-P. Liu, *Introduction to Modern Digital Holography with MATLAB* (Cambridge University, 2014).
2. J. Rosen and G. Brooker, "Digital spatially incoherent Fresnel holography," Opt. Lett. **32**(8), 912–914 (2007).
3. J. Rosen, N. Siegel, and G. Brooker, "Theoretical and experimental demonstration of resolution beyond the Rayleigh limit by FINCH fluorescence microscopic imaging," Opt. Express **19**(27), 26249–26268 (2011).
4. R. Kelner and J. Rosen, "Spatially incoherent single channel digital Fourier holography," Opt. Lett. **37**(17), 3723–3725 (2012).
5. J. Hong and M. K. Kim, "Single-shot self-interference incoherent digital holography using off-axis configuration," Opt. Lett. **38**(23), 5196–5199 (2013).
6. Z. Zhu and Z. Shi, "Self-interference polarization holographic imaging of a three-dimensional incoherent scene," Appl. Phys. Lett. **109**(9), 091104 (2016).
7. X. Quan, O. Matoba, and Y. Awatsuji, "Single-shot incoherent digital holography using a dual-focusing lens with diffraction gratings," Opt. Lett. **42**(3), 383–386 (2017).
8. T. Tahara, T. Kanno, Y. Arai, and T. Ozawa, "Single-shot phase-shifting incoherent digital holography," J. Opt. **19**(6), 065705 (2017).
9. C. M. Nguyen, D. Muhammad, and H.-S. Kwon, "Spatially incoherent common-path off-axis color digital holography," Appl. Opt. **57**(6), 1504–1509 (2018).
10. T. Nobukawa, T. Muroi, Y. Katano, N. Kinoshita, and N. Ishii, "Single-shot phase-shifting incoherent digital holography with multiplexed checkerboard phase gratings," Opt. Lett. **43**(8), 1698–1701 (2018).
11. A. Vijayakumar, Y. Kashter, R. Kelner, and J. Rosen, "Coded aperture correlation holography-a new type of incoherent digital holograms," Opt. Express **24**(11), 12430–12441 (2016).
12. A. Vijayakumar and J. Rosen, "Interferenceless coded aperture correlation holography-a new technique for recording incoherent digital holograms without two-wave interference," Opt. Express **25**(12), 13883–13896 (2017).
13. A. Vijayakumar, Y. Kashter, R. Kelner, and J. Rosen, "Coded aperture correlation holography system with improved performance [Invited]," Appl. Opt. **56**(13), F67–F77 (2017).

#331295 https://doi.org/10.1364/OE.26.018143
Journal © 2018 Received 9 May 2018; revised 17 Jun 2018; accepted 17 Jun 2018; published 28 Jun 2018

Optics EXPRESS

14. M. Ratnam Rai, A. Vijayakumar, and J. Rosen, "Single camera shot interferenceless coded aperture correlation holography," Opt. Lett. **42**(19), 3992–3995 (2017).
15. R. W. Gerchberg and W. O. Saxton, "A practical algorithm for the determination of phase from image and diffraction plane pictures," Optik (Stuttg.) **35**(2), 227–246 (1972).
16. M. R. Rai, A. Vijayakumar, and J. Rosen, "Extending the field of view by a scattering window in an I-COACH system," Opt. Lett. **43**(5), 1043–1046 (2018).
17. M. Kumar, A. Vijayakumar, and J. Rosen, "Incoherent digital holograms acquired by interferenceless coded aperture correlation holography system without refractive lenses," Sci. Rep. **7**(1), 11555 (2017).
18. J. W. Goodman, *Introduction to Fourier Optics* (McGraw-Hill, 1968).
19. A. B. VanderLugt, "Signal detection by complex spatial filtering," IEEE Trans. Inf. Theory **IT-10**, 139–145 (1964).
20. J. L. Horner and P. D. Gianino, "Phase-only matched filtering," Appl. Opt. **23**(6), 812–816 (1984).
21. T. Kotzer, J. Rosen, and J. Shamir, "Multiple-object input in nonlinear correlation," Appl. Opt. **32**(11), 1919–1932 (1993).
22. M. Fleisher, U. Mahlab, and J. Shamir, "Entropy optimized filter for pattern recognition," Appl. Opt. **29**(14), 2091–2098 (1990).
23. E. Edrei and G. Scarcelli, "Memory-effect based deconvolution microscopy for super-resolution imaging through scattering media," Sci. Rep. **6**(1), 33558 (2016).
24. R. L. White, "Image restoration using the damped Richardson—Lucy method," in The Restoration of HST Images and Spectra II, R. J. Hanisch, R. L. White, Eds., 1994.
25. K. Kondo, Y. Ichioka, and T. Suzuki, "Image restoration by Wiener filtering in the presence of signal-dependent noise," Appl. Opt. **16**(9), 2554–2558 (1977).
26. P. Campisi and K. Egiazarian, eds., *Blind Image Deconvolution* (CRC Press, 2007).
27. S. Popoff, G. Lerosey, M. Fink, A. C. Boccara, and S. Gigan, "Image transmission through an opaque material," Nat. Commun. **1**(6), 81 (2010).

1. Introduction

Digital holography has several advantages over direct imaging such as 3D imaging capability with minimum camera shots, and the ability to improve imaging qualities by intermediate signal processing ability [1]. However, in most of the digital holography techniques, multiple intensity recordings are necessary in order to recover the 3D image of the object without twin image and bias terms [1]. This requirement has been precluding such digital holography techniques from recording dynamic scenes changed at rates closer to the camera rate. Fresnel incoherent correlation holography (FINCH), a well-known incoherent digital holography technique requires at least three intensity recordings to remove the twin image and the bias terms [2,3]. The single shot capability in systems of incoherent digital holography has been accomplished by an off-axis configuration and with added complexity in the optical configuration [4–10]. Fourier incoherent holography technique published in 2012 [4] has the single shot capability but has a relatively complex optical configuration compared to FINCH. Other well-established single camera shot holography techniques include off-axis self-interference digital holography [5], self-interference polarization holographic imaging [6], incoherent digital holography with a dual focusing lens and diffraction gratings [7], phase-shifting incoherent digital holography technique [8], off-axis color digital holography [9] and phase-shifting incoherent digital holography with multiplexed checkerboard phase gratings [10]. However, various characterizations are traded-off, or complicated hardware is introduced, in order to claim the single shot capability.

A generalized incoherent digital holography technique called coded aperture correlation holography (COACH) was developed recently as a solution to the lower axial resolution of FINCH [11]. Later, it was discovered in COACH that the 3D information of the object is encoded not only in the phase but also in the intensity of the light modulated by the pseudorandom coded phase mask (CPM). Therefore, two-beam interference is not necessary in the case of COACH in order to record and reconstruct the 3D image of the object. The simplified version of COACH without two-wave interference is termed interferenceless COACH (I-COACH) [12]. The optical configuration of I-COACH is as simple as that of a direct imaging system. Without interference requirements in I-COACH systems, there is no need for vibration isolation, intensity matching between the interfering beams, phase-shifting between the multiple hologram recordings and the optical power efficiency is higher.

Optics EXPRESS

However, even in I-COACH, at least two intensity recordings are necessary, to synthesize bipolar holograms for both the object and for the point object. This is because a cross-correlation between two positive real functions produces background noise higher than a cross-correlation between two bipolar functions. The averaging technique developed for COACH for background noise suppression is necessary for I-COACH as well [13]. For specific experimental conditions such as the reflective illumination, numerous intensity recordings are required, resulting in a poor time resolution [12,13]. Recently, a modified I-COACH technique called single camera shot I-COACH (SCS-I-COACH) was developed for improved background noise suppression [14]. One of the reasons for the relatively high background noise in I-COACH was that the relationship between the CPM plane and the sensor plane in the experiment was not the Fourier relation assumed by the Gerchberg-Saxton algorithm (GSA), with which the CPMs were synthesized [15]. In SCS-I-COACH, the Fourier relation between the two planes is satisfied accurately by adding a lens function to the phase of the CPM. Therefore, the background noise suppression was improved yielding a higher signal to noise ratio (SNR). Furthermore, in SCS-I-COACH, the aperture function was engineered accurately with diffractive optical elements to accommodate two CPMs simultaneously and to produce two intensity patterns side by side in the image sensor. Therefore, one camera shot yields two intensity patterns which are sufficient to synthesize a bipolar hologram [14]. In other words, in SCS-I-COACH, the required two temporal camera shots were replaced by two camera shots distributed in the space. However, the sharing of the sensor area between two intensity patterns in SCS-I-COACH imposed a penalty in the form of a reduced field of view (FOV).

Recently, a new technique has been developed to improve the FOV of I-COACH, but again at the expense of the time resolution [16], and therefore cannot be implemented for SCS-I-COACH. Even though SCS-I-COACH is a single-shot technique, the single shot contains two intensity patterns which reduce the FOV. Therefore, if the need for two camera shots can be really avoided in both the time and space domains, then the single-shot capability can be achieved hopefully without any penalty in the form of either limited time resolution or FOV. In this study, we introduce an adaptive computational reconstruction technique called non-linear reconstruction (NLR) for reconstructing the image only by one camera shot of a single intensity pattern. Moreover, the NLR technique does not demand any modification in the optical configuration.

The manuscript consists of four sections. In the second section, the methodology and NLR technique are presented. In the third section, experiments with different conditions to evaluate the performances of the NLR are described, followed by the conclusion in the last section.

2. Methodology

The basic optical configuration of the modified I-COACH system is shown in Fig. 1. Unlike previous I-COACH configurations [12,14,16], the present setup does not have any refractive lens [17]. The principle of I-COACH is concisely summarized in the following. An object is critically illuminated by an incoherent light source and a lens *L*. The light diffracted from the object is polarized by a polarizer *P* along the active axis of the spatial light modulator (SLM) located after *P*. On the SLM, a phase mask is displayed, which is a modulo-2π sum of the CPM synthesized by GSA and a diffractive lens with a focal length *f*. The light modulated by the SLM is recorded by an image sensor located at a distance of z_h from the SLM. The focal length f of the SLM is calculated to match the imaging equation $f = \left(1/z_s + 1/z_h\right)^{-1}$. In the training stage, an impulse response library is recorded using a point object at all possible axial locations at the vicinity of the front focal plane of the lens *L*. For 3D imaging, the object is placed within the axial boundaries of the impulse response library and the object intensity pattern is recorded only once, whereas the same CPM used in the training stage is displayed

Optics EXPRESS

on the SLM. The different planes of the object are reconstructed by a cross-correlation between the object intensity pattern and the corresponding impulse response intensity pattern.

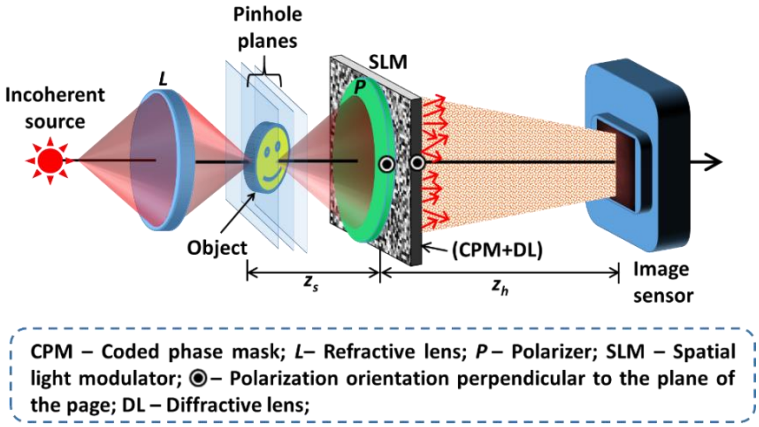

Fig. 1. Optical configuration of modified I-COACH.

Optical intensity calculations for the configuration shown in the Fig. 1 are as follows: Let us consider a point object located at $(\bar{r}_s, z_s) = (x_s, y_s, z_s)$. The light emitted from the point object has an amplitude $\sqrt{I_s}$ and the complex amplitude incident on the SLM is given by $\sqrt{I_s}\, C_0 Q(1/z_s) L(\bar{r}_s / z_s)$, where C_0 is a complex constant, Q and L represent quadratic and linear phase functions, given by $Q(a) = \exp\left[i\pi a \lambda^{-1}\left(x^2 + y^2\right)\right]$ and $L(\bar{s}/z) = \exp\left[i2\pi(\lambda z)^{-1}\left(s_x x + s_y y\right)\right]$, respectively. The complex amplitude of light modulated by the CPM and the diffractive lens of focal length f is given by $\sqrt{I_s} C_0 L(\bar{r}_s / z_s) Q(1/z_s) \exp\left[i\Phi(\bar{r})\right] Q(-1/f)$, where $\Phi(\bar{r})$ is the phase of the pseudorandom CPM calculated using the GSA and $Q(-1/f)$ represents the diffractive lens. The light diffracted from the SLM is incident on the image sensor. The complex amplitude at the image sensor is given as a convolution of $\sqrt{I_s} C_0 L(\bar{r}_s / z_s) Q(1/z_s) \exp\left[i\Phi(\bar{r})\right] Q(-1/f)$ with $Q(1/z_h)$. Therefore, the intensity pattern on the image sensor which is the point spread hologram (PSH) is given as,

$$I_{PSH}(\bar{r}_0; \bar{r}_s, z_s) = \left| \sqrt{I_s} C_0 Q\left(\frac{1}{z_s}\right) L\left(\frac{\bar{r}_s}{z_s}\right) \exp\left[i\Phi(\bar{r})\right] Q\left(-\frac{1}{f}\right) * Q\left(\frac{1}{z_h}\right) \right|^2, \qquad (1)$$

where the symbol * denotes a two-dimensional convolution and $\bar{r}_0 = (u, v)$ is the transverse location vector on the image sensor plane. Substituting the value of f from the imaging equation yields,

$$I_{PSH}(\bar{r}_0; \bar{r}_s, z_s) = \left| \sqrt{I_s} C_0 L\left(\frac{\bar{r}_s}{z_s}\right) \exp\left[i\Phi(\bar{r})\right] Q\left(-\frac{1}{z_h}\right) * Q\left(\frac{1}{z_h}\right) \right|^2. \qquad (2)$$

Equation (2) expresses the intensity distribution on the back focal plane of a spherical positive lens with a focal length of z_h, where the CPM is attached to the lens and both components are illuminated by a tilted plane-wave. It is well-known [18] that the resulting intensity is related to a scaled 2D Fourier transform of the CPM, as the following,

Optics EXPRESS

$$I_{PSH}\left(\bar{r}_0;\bar{r}_s,z_s\right)=\left|\nu\left[\frac{1}{\lambda z_h}\right]\Im\left\{\sqrt{I_s}C_0L\left(\frac{\bar{r}_s}{z_s}\right)\exp\left[i\Phi\left(\bar{r}\right)\right]\right\}\right|^2,$$
$$=I_{PSH}\left(\bar{r}_0-\frac{z_h}{z_s}\bar{r}_s;0,z_s\right), \tag{3}$$

where $\Im$ is the Fourier transform operator and ν is the scaling operator given as $\nu[\alpha]f(x) = f(\alpha x)$. Equation (3) shows that the intensity on the sensor plane is a shifted version of the intensity response for a point object located on the optical axis $\left(\bar{r}_s=0\right)$. The size of the shift from the optical axis is $\bar{r}_s\, z_h/z_s$.

A 2D object located at the same distance z_s from the lens L_1 and illuminated by a spatially incoherent light can be considered as a collection of N uncorrelated point objects given by

$$o\left(\bar{r}_s\right)=\sum_j^N a_j\delta\left(\bar{r}-\bar{r}_{s,j}\right). \tag{4}$$

The intensity response on the sensor plane for the object in the input is a sum of all the shifted point responses, as follows,

$$I_{OBJ}\left(\bar{r}_0;z_s\right)=\sum_j a_j I_{PSH}\left(\bar{r}_0-\frac{z_h}{z_s}\bar{r}_{s,j};0,z_s\right), \tag{5}$$

since $I_{OBJ}\left(\bar{r}_0;z_s\right)$ and $I_{PSH}\left(\bar{r}_0;z_s\right)$ are both positive real pseudorandom functions with dominant bias terms, the cross-correlation between them yields an undesired background noise distribution. In the past, in order to eliminate the bias terms, and the background distribution, three, or at least two, intensity patterns with different CPMs, were recorded and combined to yield a bipolar or complex holograms [12,14,16,17]. The two CPMs were selected such that their cross-correlation is negligible compared to their autocorrelation. As a result, single camera shot was not possible in I-COACH imaging systems.

To successfully reconstruct the object from a single camera shot, let us formulate the intensity response of Eq. (5) as a problem of optical pattern recognition [19–22]. The distribution given by Eq. (5) can be considered as the observed scene in which the interesting patterns I_{PSHS}s are distributed according to the shape of the input object. The reconstruction process is done by correlating I_{OBJ} with a reconstructing function calculated from I_{PSH}, whereas the goal is to obtain a correlation peak, as sharpest as possible, at every position of I_{PSH} over the entire response I_{OBJ}. Based on previous studies [11–13], it is clear that I_{PSH} itself is not the optimal reconstructing function since the cross-correlation between I_{OBJ} and I_{PSH} is equivalent to the use of a matched filter in optical pattern recognition [19], which yields sub-optimal autocorrelation peaks [20–22]. The reconstruction results shown with a phase-only filter [20] are better than that of the matched filter but still they are not optimal.

In a search for an optimal reconstruction process, we consider the case of a single object point at $\bar{r}_s$ for which the reconstructed image function should be as close as possible to $\delta\left(\bar{r}_0-z_h\bar{r}_s/z_s\right)$, in order to guarantee an optimal reconstruction. In addition, the spatial spectrum domain is studied, where the Fourier transform of the cross-correlation $\tilde{C}$ is a product of the Fourier transforms of the object function and of the reconstructing function as follows,

$$\tilde{C}=\Im\left\{I_{OBJ}\otimes I_{REC}\right\}$$
$$=\tilde{I}_{OBJ}\tilde{I}_{REC}^*=\tilde{I}_{PSH}\exp\left(i2\pi z_h\bar{r}_s\cdot\bar{\nu}/z_s\right)\tilde{I}_{REC}^* \tag{6}$$

Optics EXPRESS

where the symbol $\otimes$ denotes a correlation operation, $\bar{\nu}=(\nu_x,\nu_y)$ is the spatial frequency coordinates, $\tilde{I}_{OBJ}=\Im\{I_{OBJ}\}$, $\tilde{I}_{PSH}=\Im\{I_{PSH}\}$ and $\tilde{I}_{REC}=\Im\{I_{REC}\}$. In order to have an optimal reconstruction for a point object, *C* should be as close as possible to $\delta(\bar{r}_0-z_h\bar{r}_s/z_s)$, or $\tilde{C}$ must be as close as possible to a $constant\times\exp(i2\pi z_h\bar{r}_s\cdot\bar{\nu}/z_s)$, which can be achieved by choosing $\arg\{\tilde{I}_{REC}\}=\arg\{\tilde{I}_{PSH}\}$. Under this last condition, the reconstruction spectrum can be expressed as

$$\tilde{C}=\left|\tilde{I}_{PSH}\right|\exp(i2\pi z_h\bar{r}_s\cdot\bar{\nu}/z_s)\left|\tilde{I}_{REC}\right|. \tag{7}$$

The condition $\left|\tilde{I}_{REC}\right|=\left|\tilde{I}_{PSH}\right|$ means that the spatial filter is the matched filter with a high background noise and a relatively wider correlation peak. To optimize the reconstruction process, the magnitudes $\left|\tilde{I}_{OBJ}\right|$ and $\left|\tilde{I}_{REC}\right|=\left|\tilde{I}_{PSH}\right|$ are varied to the power of *o* and *r*, respectively. The parameters *o* and *r* are chosen to tune the power spectrum of the object and reconstructing functions, respectively. The Fourier transform of the cross-correlation given by Eq. (6) and (7) becomes,

$$\tilde{C}=\left|\tilde{I}_{PSH}\right|^{o}\exp(i2\pi z_h\bar{r}_s\cdot\bar{\nu}/z_s)\left|\tilde{I}_{PSH}\right|^{r}. \tag{8}$$

The power of $o\neq1$ on the magnitude of the object spectrum makes the reconstruction process non-linear for a multiple-point object [21]. Apparently, this non-linearity in the reconstruction process improves the SNR of the reconstructed images without losing the shift invariance of the linear correlation. The property of shift invariance is maintained because the location of each object point is encoded in the phase of $\tilde{I}_{OBJ}$, whereas the parameter *o* operates only on the magnitude and not on the phase of $\tilde{I}_{OBJ}$. Theoretically, the values of *o* and *r* that yield the sharpest image point are the values that satisfy the equation *o* + *r* = 0. However, the noisy experimental environment yields different optimal parameters that do not follow this equation. Therefore, by searching the optimal *o* and *r* in the range of [-1,1], which for *r* is the range between inverse filter (*r* = –1) to the matched filter (*r* = 1), an optimal reconstruction result can be obtained. In order to choose the optimal parameters automatically in the range $(o,r)\in[-1,1]$ a blind figure-of-merit is required. In the present case, entropy is chosen as the figure-of-merit, since the entropy has been demonstrated to be efficient to yield sharp autocorrelation peaks in pattern recognition [22]. Entropy is a measure of the disorder in a system, which in this case, is maximized when the magnitude of the reconstructed image is distributed over the entire image plane and minimized when the entire image points are accumulated in the smallest area as possible. Therefore, a minimum entropy is expected to yield the optimal reconstruction with the highest SNR. The entropy corresponding to the intensity-normalized distribution function ϕ of the output reconstructed matrix *R*(*m*,*n*), where *m*,*n* are the pixel coordinates of the image, is,

$$S(\alpha,\beta)=-\sum_M\sum_N\phi(m,n)\log[\phi(m,n)], \tag{9}$$

and $\phi(m,n)$ is defined by,

$$\phi(m,n)=\frac{\left|R(m,n)\right|}{\sum_M\sum_N\left|R(m,n)\right|}. \tag{10}$$

Optics EXPRESS

After finding the pair (*o*,*r*) which yield the minimum entropy, they are used for the reconstruction of the images. From our experience, depending upon the experimental conditions and the tested objects, the optimal values of *o* and *r* vary from case to case. Due to this behavior, the reconstruction procedure can be considered as adaptive to the experimental conditions.

3. Experiments and results

Various experiments were carried out in order to evaluate the performances of I-COACH with NLR, whereas different objects such as transmissive and reflective objects were tested.

3.1 I-COACH with transmissive objects

The experimental setup for imaging transmissive objects is shown in Fig. 2. The setup consists of two illumination channels with identical light emitting diodes (LEDs) (Thorlabs LED635L, 170 mW, central wave length of λ = 635 nm, $\Delta\lambda$ = 15 nm). The light from the LED critically illuminates the object and propagates through the beam splitter BS_1 which combines the light from the two channels. The polarizer *P* polarizes the light along the orientation of the active axis of a spatial light modulator (SLM) (Holoeye PLUTO, 1920 × 1080 pixels, 8 μm pixel pitch, phase-only modulation) located at a distance of approximately 20 cm from the object. On the SLM, a phase mask is displayed whereas its phase is the sum of the CPM phase and the quadratic phase with a focal length of f = 10 cm for a central wavelength of 635 nm. The light modulated by the SLM is collected by an image sensor (Thorlabs DCC3240M CMOS, pixel pitch = 5.3 μm, 1280 × 1024 pixels) located at a distance of approximately 20 cm from the SLM.

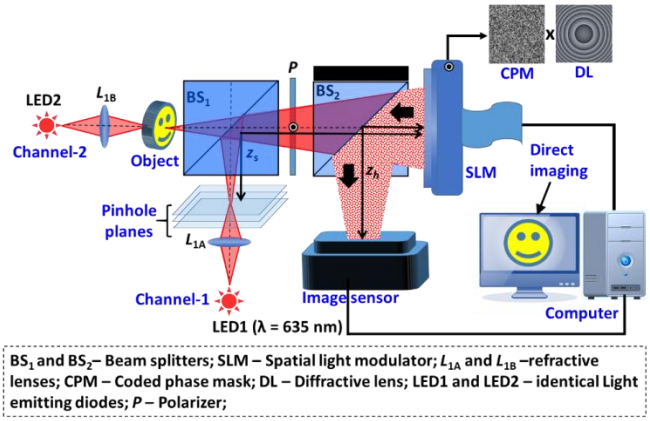

Fig. 2. Experimental setup of I-COACH with two illumination channels.

The setup is trained in the first step using a pinhole with a diameter of 80 μm in one of the optical channels and a PSH library is created corresponding to different axial locations. Unlike the previous I-COACH versions [12,17] which require at least two or more camera shots, only one camera shot is necessary at every new axial location of the pinhole resulting in a faster training stage. After the training stage, a digit '8' from National Bureau of Standards (NBS) resolution target (Thorlabs) is mounted at a distance of 20 cm from the SLM and the object hologram is recorded. The images of the PSH and object hologram recorded for the object distance of 20 cm are shown in Figs. 3(a) and 3(b), respectively. The image of the object is reconstructed using the following equation,

$$I_{IMG} = \Im^{-1}\left\{\left|\tilde{I}_{OBJ}\right|^{o}\exp\left[i\cdot\arg\left(\tilde{I}_{OBJ}\right)\right]\left|\tilde{I}_{PSH}\right|^{r}\exp\left[-i\cdot\arg\left(\tilde{I}_{PSH}\right)\right]\right\}. \qquad (11)$$

Optics EXPRESS

The different reconstructions obtained when *o* and *r* are varied from –1 to + 1 in steps of 0.1 are shown in Fig. 4. The reconstruction result corresponding to the least normalized entropy (= 1) is indicated by a red square in Fig. 4. The reconstruction results for phase-only, inverse and matched filters are indicated by yellow, pink and blue squares, respectively. Matched and inverse filters do not produce any recognizable image of the object. Phase-only filter reconstructs the image, but it is noisier compared to the case with minimum entropy produced by the NLR technique. This reinstates that matched, inverse and phase-only filters are not the optimal reconstructing functions in the case of I-COACH.

As entropy is a blind figure-of-merit, the reconstruction procedure can be automated with a rigorous search algorithm and the best reconstruction corresponding to the least entropy can be obtained within a fewer iterations than running through all the values between –1 and + 1. The rigorous search algorithm will follow the direction of decrease in the entropy along the variation in the values of *o* and *r* and therefore can find the optimal parameters relatively quickly.

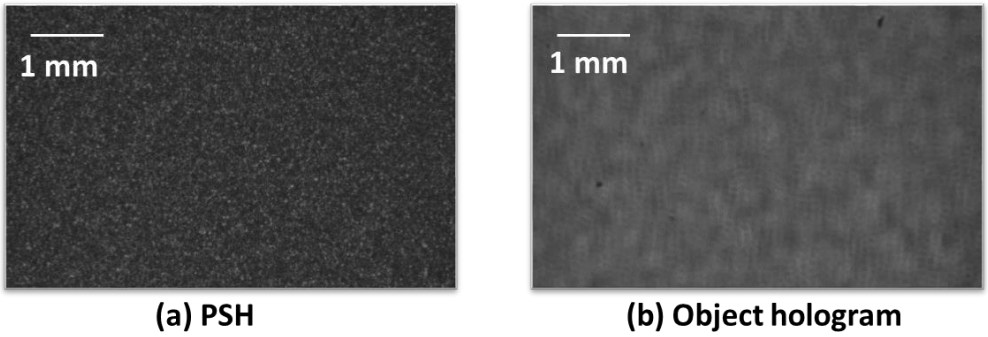

Fig. 3. Images of (a) PSH and (b) Object hologram.

Following the training stage, a two-plane object is constructed using the same object (Group 1 element 6 with 3.15 *lp/mm*) from United States Air Force (USAF) resolution target in the two optical channels. In channel 1, the digit '6' is illuminated, while in channel 2 the horizontal and vertical gratings nearby the digit '6' are illuminated. Direct imaging along the two channels at the same time produces an image consisting of the digit '6' as well as the horizontal and vertical gratings. The thickness of the two-plane object is varied in steps of 4 *mm* from $\Delta z = 0$ *mm* to 12 *mm* by moving the gratings away from the digit '6' while keeping the position of the digit constant. The reconstruction results for different thicknesses of the two-plane object are shown in Fig. 5. In the first row, one can see the reconstruction results for PSH recorded at the same distance of 20 cm from the SLM, and for the four thickness values of the object. In the second row, one sees the reconstruction results using PSHs recorded at every location of the gratings for the four thickness values. From the figures, it can be noticed that the case of minimum entropy occurs for different values of *o* and *r*, for every case, and hence the NLR is adaptive to different illumination and noise conditions. As a result, even for different experimental conditions, the object image can be reconstructed from a single camera shot. However, the background noise present in the NLR results with optimal values of *o* and *r* of the two plane objects is higher than that of the single plane object due to the involvement of more optical power. The reconstruction results demonstrate the competence of the NLR procedure for reconstructing two-plane objects with SNR of the same order of the non-averaged reconstruction results obtained using matched filter [11] and phase-only filter [13,14] with two or more camera shots in previous I-COACH versions. Moreover, the NLR technique does not demand any compromise of another imaging characteristic of I-COACH as seen in [14], where the single-shot capability is traded-off with two-thirds of the FOV of the imaging system.

Optics EXPRESS

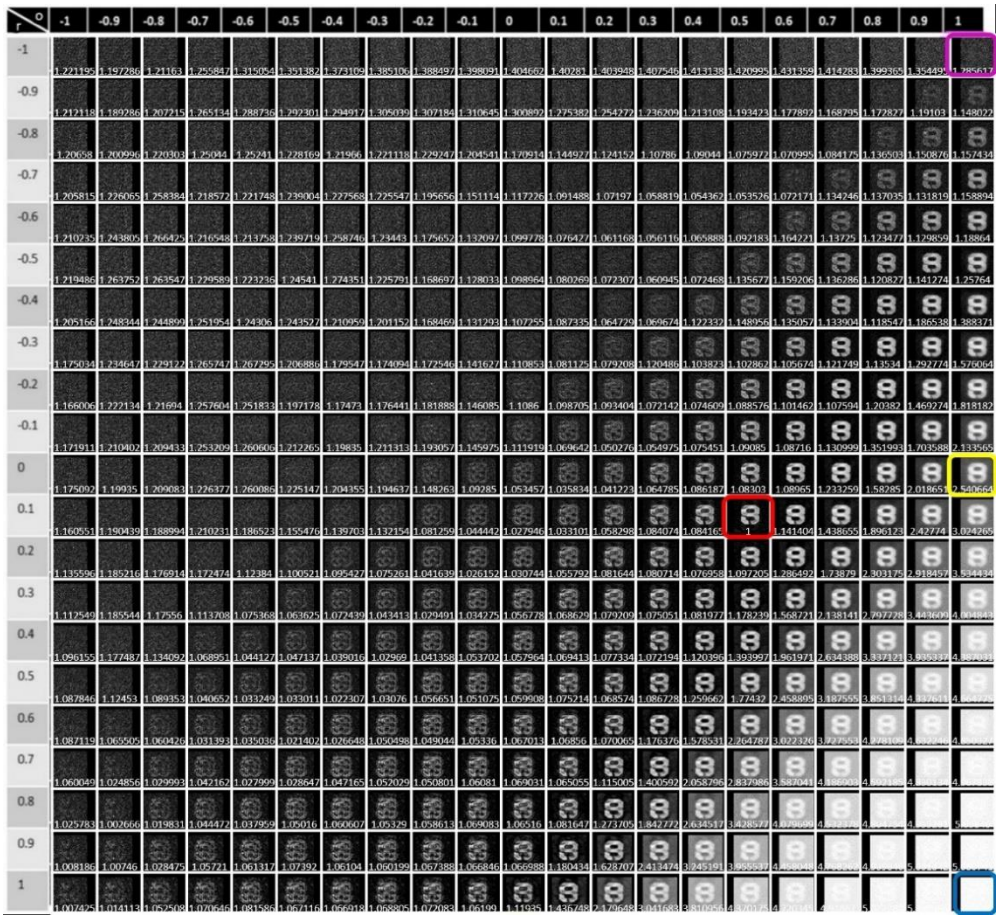

Fig. 4. Reconstruction results with the NLR procedure. The red box shows the reconstruction results with minimum normalized entropy (= 1). The blue, yellow and pink boxes show the reconstruction results with matched, phase-only and inverse filters, respectively.

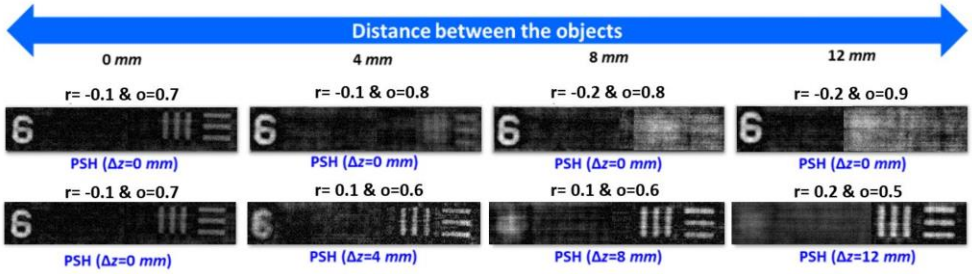

Fig. 5. Reconstruction results for the two-plane object using the NLR procedure. Row 1: Reconstruction results by PSH (Δz = 0). Row 2: Reconstruction results using PSH (Δz = 0, 4, 8 and 12 mm, respectively) matching with the axial location of the gratings.

The reconstruction results of the NLR technique are compared with the well-known deconvolution technique based on the Richardson-Lucy iterative algorithm (RLA) [23]. The RLA technique needs the library of point spread functions recorded along different axial planes similarly to the I-COACH technique. The RLA method follows a statistical approach of the Poisson statistics. Consequently, the result is not definite but probabilistic and depends on various parameters such as number of iterations and object's nature.

Optics EXPRESS

The RLA technique has been implemented to the holograms recorded using I-COACH setup of Fig. 2. The reconstructed results of the RLA technique for 50, 100, 150, 250 and 500 iterations are shown in Figs. 6(a)-6(e), respectively. It can be seen that the reconstructed images using RLA do not contain sharp edges and details of the object as obtained in the reconstruction result of NLR shown in Fig. 6(f). This comparison proves the advantage of the NLR technique over the RLA technique.

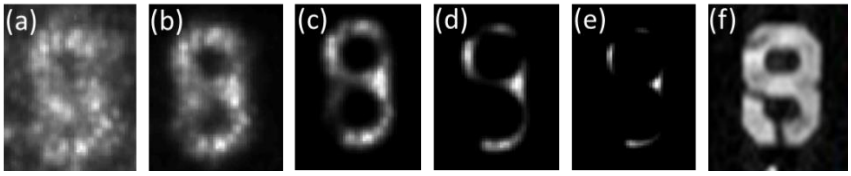

Fig. 6. Reconstruction results of RLA after (a) 50, (b) 100, (c) 150, (d) 250, (e) 500 iterations. (f) The reconstruction result of NLR technique with the least entropy value.

Moreover, RLA technique becomes unstable in the presence of noise and gives rise to artifacts and spurious signals [23,24]. To validate this, the RLA technique was implemented on the holograms recorded for a larger object made up of the digit '6' and the gratings separated laterally by a larger distance than in Fig. 5. The reconstruction results of RLA with 200, 500 and 1000 iterations are shown in Figs. 7(a)-7(c), respectively and the NLR result for minimum entropy is shown in Fig. 7(d). From Fig. 7, the advantages of NLR are evident.

The NLR method yields better reconstruction results than at least the RLA, because the algorithm automatically chooses two critical parameters o and r whose role is to balance between two contradict requirements; the desire to reconstruct each object point as sharpest as possible and to suppress the noise on the image plane as much as possible. The first requirement is fulfilled for $o + r = 0$, whereas the second one is satisfied in the case of the matched filter where $o = r = 1$. Indeed, the optimal parameters o and r in many experiments have been found always within the region $o + r > 0$, $r \leq 1$ and $o \leq 1$. Moreover, the parameters o and r are adaptive to the realistic noise in the setup and to the scattering rank of the CPM used.

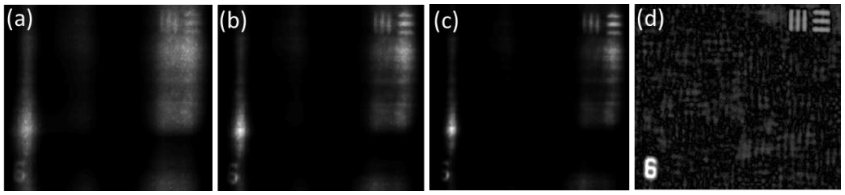

Fig. 7. Reconstruction results of RLA with (a) 200, (b) 500, (c) 1000 iterations, and (d) reconstruction result of the NLR technique.

3.2 I-COACH with reflective objects

The experiment was repeated for reflective objects printed by a white ink on a black background. A digit '*B*' of the size of 2 × 1.2 *mm* is mounted in one of the optical channels. The experimental setup is shown in Fig. 8. The light diffracted from the object is modulated by the SLM located at a distance of 15.5 *cm*. The light modulated by the SLM is incident on the image sensor located at a distance of 10.5 *cm* from the SLM. On the SLM, we display a phase mask obtained by a phase addition of the diffractive lens phase with a focal length of 6.5 *cm* and the CPM phase. The object holograms are recorded for the same object at different axial locations with a separation of 1.8 *cm* and reconstructed by the NLR using the PSHs recorded at the two axial locations. The images of the object holograms and the corresponding PSHs at the two axial locations are shown in Fig. 9. The reconstruction results of the two object holograms using the two PSHs are shown in Fig. 10, whereas the two parameters (o,r) of the NLR are specified on each figure.

Optics EXPRESS

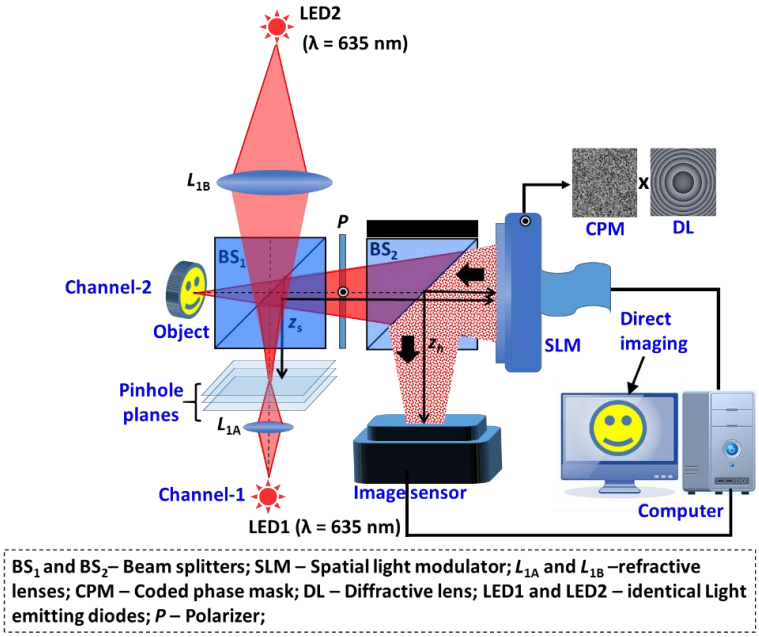

Fig. 8. Experimental setup of I-COACH with object illumination in reflection mode.

Recalling the previous studies on imaging reflective objects using I-COACH [12] and LI-COACH [17], 60 and 40 camera recordings were respectively necessary to reconstruct the objects. Due to the adaptability of NLR technique, a single camera shot is now sufficient to reconstruct a reflective object. In comparison to transmissive objects the reconstruction results have lower SNR, due to a lower object contrast (signal to background ratio) and lower object intensity of the reflective target.

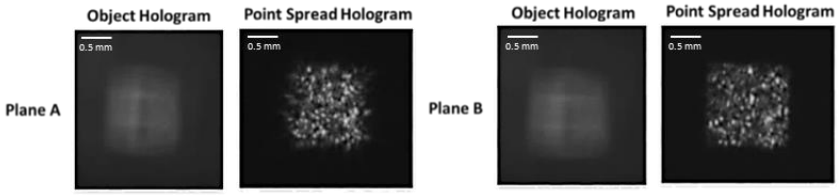

Fig. 9. Images of object holograms and point spread holograms in planes A and B separated by a distance of 1.8 cm.

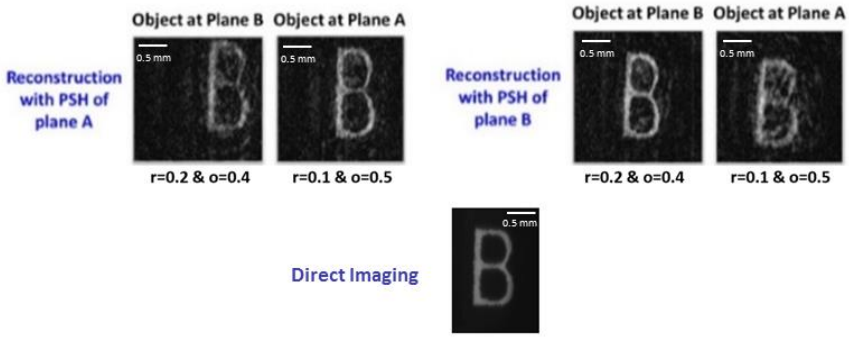

Fig. 10. Reconstruction results of the two object holograms using the two different PSHs and direct imaging.

Optics EXPRESS

4. Summary and conclusions

An adaptive digital reconstruction technique termed NLR has been developed for reconstruction of 3D images with a single camera shot of the I-COACH system. The NLR technique has been implemented with different experimental conditions such as transmission and reflection modes of illumination. The reconstruction results for the different cases clearly demonstrate the adaptability of the technique. To obtain the reconstruction results over the entire range of $(o,r)\in[-1,1]$ in steps of 0.1, requires a total of 443 Fourier transforms which may increase the image reconstruction duration. However, rigorous search algorithms can be developed to limit the search only along the direction of decrease of the entropy, and might reduce the number of iterations.

In this preliminary work, the NLR is only compared to RLA. However, in the future, the NLR should be compared to other noise-handling deconvolution methods such as Wiener deconvolution [25], and regularization methods [26,27]. The NLR reconstruction was tested for various levels of noise on the camera plane, whereas the noise was increased by increasing the scattering rank of the CPM. It has been found that by gaining the scattering by 10% (from the entire range of the rank) increases the optimal parameters o and r by 5% (from their entire range) in average, towards the matched filter ($o = r = 1$). The course towards the matched filter is understood in view of the fact that matched filter is known as the optimal linear filter for maximizing the SNR in the presence of additive stochastic noise.

The NLR has comparable results with the I-COACH of two camera shots, in which each of the correlated functions is converted from a positive intensity function to a bi-polar function. Thus, one can look on NLR as a more efficient way to effectively transform each positive captured function, the PSH and the object hologram, to a bi-polar function. The above demonstrations show that the NLR is not limited to any specific optical configuration. Hence, the NLR might work well for reconstruction of 2D and 3D images for any optical system, which involves the use of a cross-correlation between two functions.

Funding

Israel Science Foundation (ISF) (Grant No. 1669/16); Israel Ministry of Science and Technology (MOST).